

DEVELOPMENT OF GUGGULSTERONE-LOADED PHYTOSOMES: A QUALITY BY DESIGN-BASED CHARACTERIZATION AND OPTIMIZATION STUDIES

JAMAL BASHA DUDEKULA¹, JEBASTIN KOILPILLAI², DAMODHARAN NARAYANASAMY^{2*}

¹Department of Pharmacognosy, SRM College of Pharmacy, SRM Institute of Science and Technology, Kattankulathur, Chennai-603203, India. ²Department of Pharmaceutics, SRM College of Pharmacy, SRM Institute of Science and Technology, Kattankulathur, Chennai-603203, India

*Corresponding author: Damodharan Narayanasamy; Email: damodhan@srmist.edu.in

Received: 24 May 2024, Revised and Accepted: 04 Jul 2024

ABSTRACT

Objective: The primary objective of this study was to enhance drug delivery efficiency through the design and optimization of guggulsterone-pyrosomes, employing a 3-factor, 3-level box-behnken design.

Methods: The methodology involved a solvent evaporation technique utilizing guggulsterone and soy lecithin, with a systematic variation and optimization of critical factors such as soy lecithin and guggulsterone concentration, alongside temperature adjustments to refine the phytosome formulations. The characterizations of these formulations were extensive, with a particular emphasis on key quality attributes, notably percentage entrapment efficacy and drug release.

Results: The optimized guggulsterone-pyrosomes demonstrated impressive outcomes, showcasing a remarkable entrapment efficiency of 92.64% and a noteworthy drug release rate of 91.69% at 24 h. These formulations displayed heightened viability in selected cell lines, exhibiting cellular toxic concentrations ranging from 253.39 to 330.44 µg/ml. Moreover, they exhibited stability under stressed conditions from a physicochemical perspective. The particle size was measured at 137.8 nm, with a zeta potential of -25.3 mV.

Conclusion: Significantly, the extended drug release from guggulsterone-pyrosomes adhered to first-order kinetics with Fickian diffusion. In summary, this study underscores the efficacy of the box-behnken design in crafting optimized guggulsterone-pyrosomes, showcasing their potential as promising drug delivery carriers. The enhanced drug delivery platform exhibits significant promise in amplifying antihyperlipidemic effects, attributed to the improved performance and stability of these innovative phytosomes

Keywords: Phytosome, Bioavailability, Box-behnken design, Guggulsterone, Hyperlipidemia, Soy lecithin

© 2024 The Authors. Published by Innovare Academic Sciences Pvt Ltd. This is an open access article under the CC BY license (<https://creativecommons.org/licenses/by/4.0/>) DOI: <https://dx.doi.org/10.22159/ijap.2024v16i5.51559> Journal homepage: <https://innovareacademics.in/journals/index.php/ijap>

INTRODUCTION

The engineering of particulate matter into nano dimensions promises advantageous drug delivery over conventional systems. Site-specific, targeted, and controlled delivery of drugs over time with nanoparticles as the carriers enhances the efficacy and reduces the toxicity of drugs. Since its conceptualization by Dr. Richard P. Feynman in the late 1950s, nanotechnology has been gaining momentum and revolutionizing the day-to-day aspects of life, thereby simultaneously uplifting the global standards of living and economy [1]. The positive impacts are noticeable in pharmacokinetic properties and targeted delivery of drugs at the selected site for the choice of action in the treatment of chronic diseases like diabetes, cancer, etc. [2]. Big-sized particles may be a barrier to drug delivery, which might result in poor solubility, low bioavailability, instability, a diminished absorption rate, altered target-specific delivery, tonic effectiveness, and adverse effects of drugs. Phytosomes, also known as phyto-phospholipid complexes, have emerged as particularly promising carriers for enhancing the bioavailability of active phyto-constituents, as demonstrated in research [3, 4] Phytosomes serve as vesicular carriers for drug delivery, effectively augmenting the absorption and bioavailability of poorly water-soluble drugs, as evidenced by various studies [5, 6]. The process involves the complexation of natural active phyto-constituents with phospholipids. Phytosomes excel in various aspects, including greater drug encapsulation, faster absorption rates, heightened bioavailability, and enhanced stability, positioning them as superior lipid carriers compared to alternatives, as demonstrated by research [7, 8]. These innovative drug delivery carriers, known as phytosomes, have demonstrated their ability to enhance the therapeutic effects of numerous pharmaceuticals and herbal extracts. Examples include apigenin, silymarin, rutin, quercetin, curcumin, cuscuta extract, thymoquinone, and silybin]. Hyperlipidemia is a multifaceted disorder characterized by elevated

lipid levels within the human body. It precipitates a multitude of repercussions, including cardiovascular ailments, diabetes mellitus, and fatty liver disease, which collectively accounted for one-third of global fatalities by the year 2020. This condition is recognized as a prominent global health concern [9-16].

The utilization of various chemical and synthetic compounds, such as statins, fibrates, bile acid sequestrants, lipase inhibitors, and others in the management of hyperlipidemia is curtailed due to the emergence of severe side effects, encompassing myopathy, rhabdomyolysis, flatulence, bloating, and renal impairment [17]. Current research endeavors are predominantly directed towards the development of alternative, naturally-derived agents like allicin, guggul lipid, citrus flavonoids, curcumin, green tea, epigallocatechin gallate, resveratrol, and various plant extracts for the safe and efficacious management of hyperlipidemia. Notably, these natural compounds offer advantages over their chemical counterparts by being safe and associated with minimal or no adverse effects [18]. Among these options, guggulipid stands out as a noteworthy choice. Derived from the gum resin of the Ayurvedic plant known as *Commiphora mukul* (referred to as "Guggulu" in Sanskrit), it has enjoyed a long history of use in Ayurvedic medicine in India for addressing a diverse array of health conditions. These include arthritis, obesity, hyperlipidemia, and various lipid disorders [19, 20]. The active components within guggulipid, namely E and Z-guggulsterone, operate by competitively binding to the Farnesoid X Receptor (FXR). This binding action impedes the enzymatic transformation of cholesterol mediated by Cholesterol 7 alpha-hydroxylase (CYP7A1), in addition to interacting with nuclear hormone receptors responsible for bile acid regulation and cholesterol metabolism, known as Bile Acid Regulation (BAR). Consequently, these interactions lead to a direct reduction in hepatic cholesterol levels in humans [21]. Besides that, its efficacy is often compromised by low solubility and bioavailability and rapid first-

pass metabolism. Owing to the above-mentioned drawbacks, there is a need to explore new delivery systems with improved solubility and permeation bioavailability.

Employing a systematic approach utilizing a three-factor, three-level Box-behnken design. (BBD) with five center points, this study aims to optimize guggulipid phytosomes for extended drug delivery. Through the judicious utilization of the Design of Experiments (DoE), our objective is to unlock the complete therapeutic potential inherent in guggulipid, thereby offering fresh insights into its pharmacological and therapeutic effects. This marks the commencement of a journey to harness the potent forces of nature for the management of hyperlipidemia, promising a safer and more efficacious route to well-being. In the ensuing sections, we delve comprehensively into the methodologies, outcomes, and ramifications of our research, illuminating the path toward a more promising and natural future in the management of hyperlipidemia.

MATERIALS AND METHODS

Guggulsterones was acquired from M/s. Chemiloids, located in Vijayawada, India, and soy lecithin from Sigma-Aldrich in Bangalore, India. Milli Q water was employed consistently throughout this research. Furthermore, essential materials such as Fetal Bovine Serum (FBS), Dulbecco's Modified Eagle's Medium (DMEM), trypsin, dimethyl sulfoxide (DMSO), 3-(4, 5-dimethylthiazol-2-yl)-2,5-diphenyltetrazolium (MTT), and an antibiotic-antimycotic mixture were procured from Himedia, based in Mumbai, India. It is noteworthy that all other chemicals and reagents employed in this study adhered to analytical grade standards and were generally recognized as safe.

Drug-excipient compatibility studies

Compatibility studies between pure guggulsterones and excipients were conducted using Fourier Transform Infrared (FTIR) spectroscopy (Shimadzu 8300E, Japan). The FTIR spectra of guggulsterones and the physical mixture were examined by using the potassium bromide (KBr) pellet method. Each sample's spectra were generated from 32 single-average scans, employing a resolution of 4 cm⁻¹ within the absorption range of 400–4000 cm⁻¹. The acquired infrared spectra were subsequently analyzed to identify functional groups at their respective wavenumbers (cm⁻¹) [22]

Preparation of phytosomes

Precisely measured quantities of guggulsterones and soy lecithin were introduced into a 250 ml round-bottom flask and dissolved in 50 ml of methanol. Subsequently, this mixture was refluxed using a rotary evaporator, maintaining temperatures at 40/50/60 °C for 3.5 h, adhering to the requisite parameters. The resulting solution was then concentrated until complete solvent evaporation occurred. The resulting guggulsterone-soya lecithin complexes (phytosomes) were continuously stirred with n-hexane for 2 h at 40 °C. Subsequently, the hexane was eliminated through filtration, and the formed phytosomes were dried under a vacuum to eliminate any residual solvents. Finally, the Guggulsterone-Phytosomes (GPs), appearing as a thin film, were stored in an air-tight amber-colored bottle at a temperature range of 2-8 °C for further studies [19].

Design of experiment

To explore the primary, interactive, and quadratic factors, a 3-factor, 3-level BBD was employed in this study, utilizing Design Expert® (Version 13, Stat-Ease Inc., Minneapolis, USA). Quadratic response surface model and second-order polynomial models were employed to evaluate and optimize the GPs. Based on preliminary investigations, the quantities of guggulsterone (X1), soy lecithin (X2), and temperature (X3) were selected as independent variables, each examined at three distinct levels: low (-1), medium (0), and high (+1). As for the responses, percentage Entrapment Efficiency (EE, Y1) and percentage Drug Release (DR, Y2) were chosen with specific constraints. The Design Expert software facilitated the creation of seventeen experimental runs, all executed in a randomized fashion to mitigate potential sources of bias. The non-linear quadratic model generated by the BBD is as follows:

$$Y = b_0 + b_1X_1 + b_2X_2 + b_3X_3 + b_{12}X_1X_2 + b_{13}X_1X_3 + b_{23}X_2X_3 + b_{11}X_1^2 + b_{22}X_2^2 + b_{33}X_3^2 \quad (1)$$

In this context, Y denotes the recorded response corresponding to each combination of factor levels, with b₀ serving as the intercept. The coefficients b₁ to b₃₃ are determined based on the observed experimental values of Y. Furthermore, X₁, X₂, and X₃ represent the coded levels of the independent variables. The terms X₁X₂ represent the interaction terms to study the response to the simultaneous change of three factors and quadratic terms to investigate the non-linearity, respectively. To assess the significance and influence of each factor, as well as their interactions, on the response variables, employed statistically significant coefficients, R-square values, as well as two-dimensional (2D) contour and three-dimensional (3D) response surface plots. The quadratic polynomial equation, utilized for statistical validation, was derived through Analysis of Variance (ANOVA). For the optimization of GPs, a numerical optimization technique was employed, coupled with a desirability approach [12, 19].

Drug product (GPs) characterization

Morphology, particle size, and electrokinetic potential

The morphology and structural characteristics of the optimized GPs were meticulously examined using a Transmission Electron Microscope (TEM-100S Microscope). Samples were diluted with ethanol in a ratio of 1:20 and sonicated for 10 min. A drop of phytosome was fixed onto a carbon-glazed grid and left to form a thin film. The phytosome pictures were taken using TEM. [19, 20]. Furthermore, the particle size and electrokinetic potential of the GPs in the optimized formulation were evaluated employing a Zetasizer (Horiba SZ-100). These measurements were conducted through the dynamic light scattering technique, with a scattering angle of 90° and a constant temperature of 25±0.5 °C [19].

Determination of entrapment efficiency

A precisely measured quantity of 25 mg of phytosomes was dissolved in methanol and subsequently diluted. The absorbance of the solution was then recorded at 254 nm to ascertain the concentration of guggulsterones within the solution [23]. Based on this determination, the total yield of guggulsterones was calculated, and the Entrapment Efficiency (EE) was subsequently determined using the following formula,

$$EE(\%) = \frac{\text{Amount of guggul in phytosomes}}{\text{Total amount of guggul taken}} \times 100 \dots\dots (2)$$

Solid state characterization (XRD and DSC)

X-ray Diffraction (XRD) patterns were obtained for guggulsterones, soy lecithin, and the optimized GPs using an X-ray diffractometer (Horizon, Chennai). These measurements were conducted at room temperature, applying a voltage of 30 kV, a current of 5 mA, and a scanning speed of 4°/min. The samples were subjected to scanning within the 5 to 50° (2θ) range, with a step size of 0.01° and an interval of 0.1 sec [20]. Additionally, thermograms of guggulsterones, soy lecithin, and the optimized GPs were recorded utilizing a Differential Scanning Calorimeter (DSC-60, Shimadzu). The thermal behaviour was investigated by heating 2 mg of each sample at a rate of 10 °C per minute, ranging from 25 °C to 400 °C, within a covered sample pan while maintaining a nitrogen purge at a rate of 60 ml/min [24].

In vitro drug release study

The *in vitro* release of guggulsterone from GPs was evaluated employing a dynamic dialysis method characterized by a Molecular Weight Cut-Off (MWCO) in the range of 12,000–14,000 g/mol and pore size of 2.4 nanometers. Subsequently, these bags were immersed in a 500 ml buffer solution with a pH of 7.4, maintained at a temperature of 37±1 °C, while a paddle rotation speed of 50 rpm was maintained. At predetermined intervals, 5 ml aliquots were withdrawn and promptly replaced with an equal volume of buffer solution. The concentration of guggulsterone in these aliquots was measured at 254 nm using a Shimadzu UV-1800 spectrophotometer. Each experiment was conducted in triplicate, and the percentage of drug release was subsequently calculated. Moreover, the release kinetics from GPs were investigated by fitting the data to several kinetic models [21].

Optimization

The formulation variables were optimized through a numerical optimization technique to achieve the desired outcomes. To gauge

the reliability of these optimized conditions, additional experiments were replicated in triplicate. The percentage of error was computed by comparing the mean values of the experimental data with the predicted values. The acquired data were scrutinized to assess the precision and appropriateness of the conditions employed in the GPs preparation process.

Stability studies

The stability of the optimized GPs formulations was assessed through a rigorous testing regimen involving their storage at controlled temperatures of 4.0 ± 1 °C within a refrigerator and 40 ± 2 °C within a stability testing chamber over a duration spanning three months. At intervals of 0, 30, 60, and 90 days, the samples underwent thorough evaluation for various physical attributes, including appearance, consistency, the presence of clogs, or any phase separation. Additionally, critical chemical parameters such as EE and drug content were diligently monitored. It is important to note that accelerated stability studies for the optimized GPs were conducted according to the guidelines set forth by the International Conference on Harmonization (ICH) [21].

In vitro cell line studies

The compatibility and viability of the optimized GPs with cells were assessed through *in vitro* cell line studies (Cell culture and stimulation and MTT assay). The selected cell lines for this study comprised mouse fibroblasts (3T3-L1), mouse motor neuron-like cells (NSC-34), and kidney epithelial cells (Vero cells), which were procured from the National Center for Cell Sciences, Pune, India. These cells were cultured in DMEM supplemented with 10% (v/v) Bovine Calf Serum (BCS) and 1% (v/v) penicillin-streptomycin. Following two days of reaching confluence, the cells were induced to differentiate using DMEM containing 10% Fetal Bovine Serum (FBS), 0.5 mmol 3-isobutyl-1-methylxanthine (IBMX), and insulin (10 µg/ml) for an additional two days. Subsequently, the cells were maintained in a medium consisting of 10% DMEM/FBS with insulin (10 µg/ml) for another two days, followed by culturing in a 10% FBS/DMEM medium for an additional four days, resulting in over 90% of the cells differentiating into 3T3-L1 adipocytes with accumulated lipid droplets. The differentiated 3T3-L1/NSC-34 and Vero cells were then exposed to the optimized GPs. These cells were incubated at 37 °C with 5% CO₂ throughout the experiments and were initially grown and seeded at a density of 1×10^4 cells per well in 96-well plates. Subsequently, the cells were treated with GPs and incubated with MTT solution for 3 h at 37 °C. After the incubation period, the supernatants were removed, DMSO was added to each well, and the plates were agitated to dissolve the crystal product. The absorbance was then measured at 540 nm using a microplate reader (Tecan M200) [25].

Apparent water solubility

The apparent solubility was determined by treating drugs, physical mixtures, and complexes to 5 ml of water-sealed glass containers at ambient temperature. The solution was circulated for 24 h and then

centrifuged for 20 min at 1,000 rpm to eliminate the residues of the drug and complexes. Before measuring the 254 nm absorption with a UV spectrometer, 1 ml of filter material was diluted in 9 ml of distilled water and filtered through a membrane filter (0.45 µm).

Apparent octanol-water partition coefficient

The GPs were dissolved into n-octanol at a concentration of 200g/ml. The solution was mixed in a conical flask with 5 ml distilled water (pH 5.6), HCl (0.1 M, pH 1.2), or a phosphate buffer saturated with n-octanol (pH 6.8, 7.4, and 7.4) of 45 ml, each. The prepared sample was shaken in a conical container at 300 rpm and 37 °C for 24 h to achieve saturation and equilibrium. Then separate the sample into an aqueous phase and an octanol phase by separation funnel. To calculate the concentration of the drug, 1 ml of octanol phase contains GP and is taken and diluted with 9 ml of methanol. This was done by measuring the solution with UV spectrometers at 254 nm.

Statistical analysis

All experiments were conducted in triplicate, ensuring the robustness and reliability of the results. The outcomes were presented in the form of mean values accompanied by their respective standard deviations (SD). Statistical comparisons of the data were executed through both ANOVA and independent Student t-tests. The significance threshold was set at $p < 0.05$, indicating a statistically significant level for the observed differences.

RESULTS AND DISCUSSION

Drug-excipient compatibility studies

The FTIR spectra of guggulsterone, soy lecithin, and their physical mixtures are illustrated in 1. The FTIR spectrum of guggulsterone displayed distinctive absorption peaks at specific wavenumbers: 1455.05 cm⁻¹ (C=C aromatic stretching), 1700.78 cm⁻¹ (C=O stretching), 2869.39 cm⁻¹ (CH stretching), 2955.18 cm⁻¹ (C-H vibration), 3443.70 cm⁻¹ (combined peaks associated with -NH₂ and -OH), 1737.58 cm⁻¹ (C=O stretching), 1671.98 cm⁻¹ (C=C stretching), 1409.31 cm⁻¹ (CH₂ bending), as well as 1383.07, 1340.77, and 1260.96 cm⁻¹ (O-H bending). Furthermore, the spectrum exhibited peaks at 1095.11 and 1026.82 cm⁻¹ (C-F bending), 1169.51 cm⁻¹ (C-O stretch), 884.52 cm⁻¹ attributed to the distribution of aromatic protons, and 759 cm⁻¹ associated with CH₂ rocking. On the other hand, the FTIR spectrum of soy lecithin (SL) revealed peaks at 3421.92 cm⁻¹ (O-H stretching), 1620.38 cm⁻¹ (C=O stretching), and vibrational peaks at 1170.28 cm⁻¹ and 1098.87 cm⁻¹ attributable to the presence of C=O and C=C bonds [25]. Notably, the characteristic peaks observed in the FTIR spectra of guggulsterone and soy lecithin were conserved in the spectrum of the GPs. There were no abnormal peaks observed in the IR spectra of guggulsterone. This observation suggests the absence of any chemical interaction between the drug and its carrier constituents. The results suggested that there was no interaction among the excipients and between the drug-excipients.

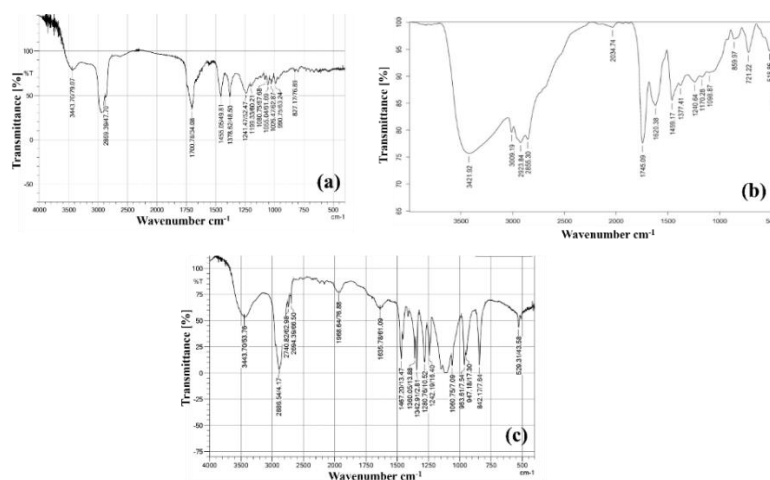


Fig. 1: FTIR of (a) Guggulsterone, (b) soy lecithin and (c) GPs

Preparation of phytosomes

The production of guggulsterone-loaded phytosomes using the solvent evaporation technique was executed successfully. The application of DoE principles, specifically a 3-factor 3-level BBD, proved to be a highly effective logistic tool for designing and optimizing promising GPs that met the desired criteria. These results provided valuable insights into the impacts of formulation variables and process parameters, facilitating the development of these promising GPs. This method is chosen for its inherent simplicity and proven effectiveness in yielding phytosomal formulations that possess the desired attributes [3]. Seventeen

formulations were prepared as per the BBD mentioned in 1. A drug-phosphatidylcholine complex refers to the association of a drug with phosphatidylcholine without dispersion. This complex exists in a non-dispersed form, where the drug is bound to the phospholipid. On the other hand, a phytosome is characterized by a dispersed drug-phospholipid complex in a dispersion medium. In this case, the complex is not only formed but is also dispersed within a medium, contributing to the unique properties of a phytosome as a lipid nanocarrier. In summary, the key distinction lies in the dispersal state: a drug-phosphatidylcholine complex is non-dispersed, while a phytosome involves the dispersion of the complex in a medium [26, 27].

Table 1: BBD generated formulation runs and their results

Run	Guggul (X ₁ , mg)	Soya lecithin (X ₂ ,mg)	Temp (X ₃ , °C)	EE (Y ₁ , %)*	DR (Y ₂ , %)*
1	150	400	50	90.07±0.25	91.05±0.68
2	100	400	40	80.72±0.91	82.45±0.36
3	150	400	50	90.79±0.74	90.88±0.43
4	150	200	40	85.12±0.11	86.03±0.80
5	200	200	50	88.51±0.86	86.84±0.94
6	200	400	60	86.73±0.38	87.63±0.43
7	150	400	50	90.56±0.07	90.56±0.90
8	100	400	60	86.44±0.46	88.26±0.48
9	100	200	50	78.28±0.83	85.08±0.33
10	150	200	60	86.57±0.71	88.23±0.61
11	150	400	50	89.65±0.59	91.39±0.73
12	150	600	40	91.74±0.60	90.18±0.51
13	150	400	50	91.02±0.27	91.47±0.77
14	200	600	50	90.0 ±0.33	91.52±0.68
15	100	600	50	87.86±0.82	88.0±0.12
16	200	400	40	91.45±0.16	88.13±0.47
17	150	600	60	92.84±0.04	92.07±0.83

*Data presented are means±SD of triplicate experiment (n=3).

Morphology, particle size, and electrokinetic potential

The optimized GPs exhibited a spherical shape, even distribution, and a slightly rough and porous texture. Furthermore, the particle size and zeta potential of these optimized GPs were measured at 137.8±1.87 nm and -25.3±0.63 mV, respectively (fig. 2). The zeta potential of Guggulsterone formulation was found to be more negative -25.3±0.63 than the pure guggulsterone, it may occur due to the net charge of the polymer and protein used for the formulations. Zeta potential, which is the surface charge, contributed to the stability of the formulation. The low value of surface charge provides stability as well as prevents the aggregation of the particles due to strong electrostatic repulsion interaction. Normally, the value of the zeta potential of -30 mV to +30 mV is considered a sufficient repulsive force to achieve better physical colloidal stability [28].

Entrapment efficiency

The optimized guggulsterone phytosomes witnessed enhanced EE and extended drug release following first-order kinetics with Fickian diffusion. The percentage EE of GPs ranged from 78.28±0.83% (F9) to 92.8±0.04 % (F17). The BBD-generated polynomial equation for EE is as follows-

$$Y_1 = 90.42 + 2.92 X_1 + 2.99 X_2 + 0.44 X_3 - 2.02 X_1 X_2 - 2.61 X_1 X_3 - 0.087 X_2 X_3 - 3.49 X_1^2 - 0.76 X_2^2 - 0.58 X_3^2 \dots (3)$$

The quadratic model exhibited highly significant statistical values, with p-values of less than 0.0001 and an F ratio of 62.32, indicating the model's significance in predicting EE. The polynomial equation associated with this model achieved an R-squared (R²) value of 0.9911, signifying a strong goodness of fit [28]. Consequently, this robust model was utilized for navigating the design space. Furthermore, the influence of all independent variables (X₁, X₂, and X₃) on %EE was elucidated through comprehensive analysis, as depicted in the 3D response surface plots and 2D contour plots showcased in fig 6. It was found that the entrapment efficiency is increasing linearly as the concentration of Guggulsterone and Soya

lecithin increases; because the medication is easily available for encapsulation, and this might be due to the increasing concentration of polymer will make the phytosomes membrane less permeable and hence promotes entrapment efficiency [29]. The temperature has a direct positive effect on the entrapment efficiency of prepared guggulsterone phytosomes an increase in temperature increases the entrapment efficacy. Fig. 6e displays the fitted polynomial equations connecting the response (entrapment efficiency, % w/w) to the altered components. Conclusions could be reached by using the polynomial equations after taking into account the coefficient's magnitude and associated mathematical sign (positive). Additionally, according to fig. 2e's results, every coefficient was statistically significant (p<0.05). The quadratic model was found to have an excellent match with a correlation coefficient (R²) of 0.9522. The positive coefficients were shown by the multiple regression analysis. This suggested that as X₃ were raised, the entrapment efficiency increased as well also increased. Based on the central composite design and response surface plots depicting the changes in the entrapment efficiency (%) as a function of X₃. The response surface plots and contour plots (fig. 6e) indicated a strong influence of the studied factors on entrapment efficiency. Increasing levels of X₃ found to be favorable conditions for obtaining higher entrapment efficiency. Since the active ingredient in the formulation is phytoactive, an increase in entrapment efficiency was seen [30].

Solid state characterization (XRD and DSC)

The XRD analysis of guggulsterones revealed a series of distinct peaks within the 2θ range of 10 to 40°, as illustrated 3. Additionally, the DSC thermograms of both Guggulsterone and the GPs are presented in 4.

The XRD studies unveiled a noteworthy shift in the characteristic peak of guggulsterone, originally occurring at 13.899°, which was subsequently displaced to 19.676° within the optimized GPs formulation. This shift in peak position strongly indicated the presence of guggulsterone in an amorphous state [30]. Additionally, in DSC

studies, an endothermic peak corresponding to guggulsterone was observed at 92.89°, and this characteristic peak remained unaltered in

the thermogram of the GPs. This observation suggested the preservation of guggulsterone's structural integrity within the GPs.

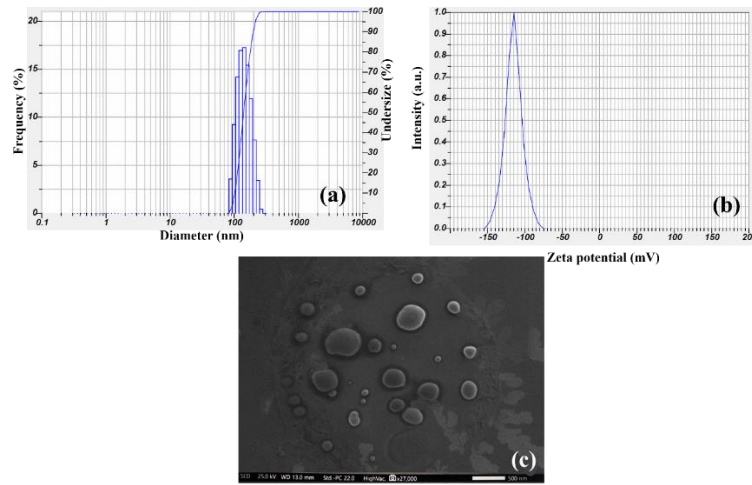


Fig. 2: Particle size (a), electrokinetic potential (b), and morphology (c) TEM of optimized

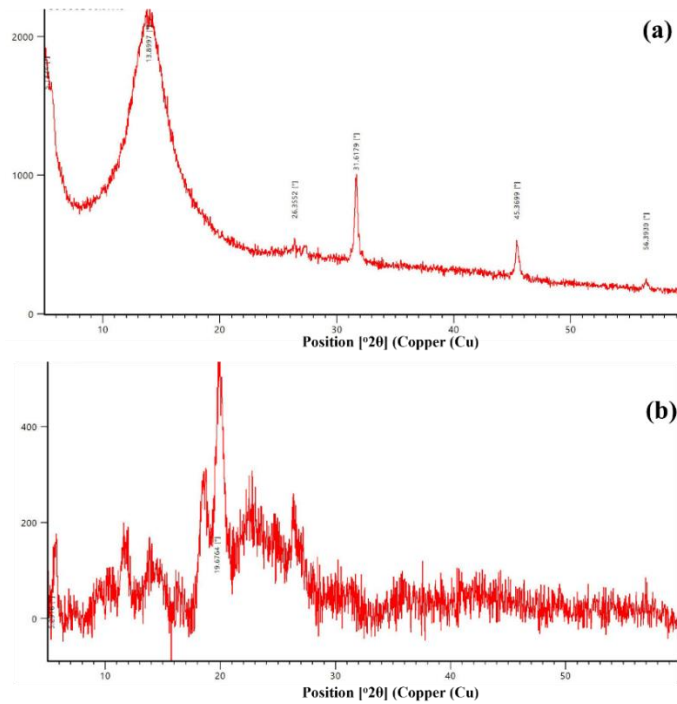


Fig. 3: XRD of (a) Guggulsterone and (b)GPs

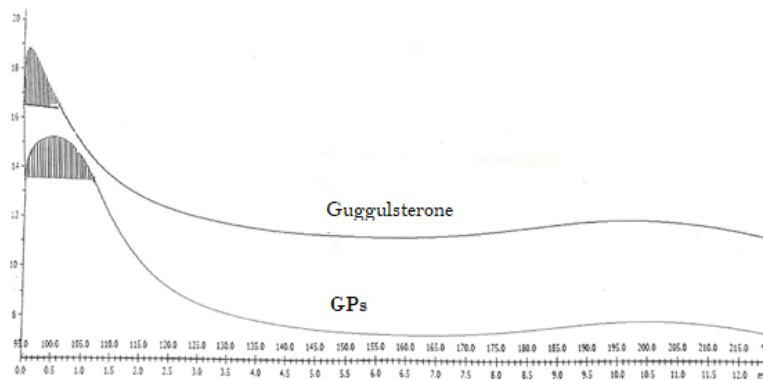


Fig. 4: DSC thermograms of guggulsterone and GPs

Drug release studies

The optimized GPs demonstrated a guggulsterone release rate $91.56 \pm 0.67\%$ after a 24 h study. The drug released from GPs was found to be slower than the pure drug because conjugation may offer double barriers on the drug released from the phytosomal formulation. To better comprehend the release kinetics of guggulsterone from the GPs, the release data were subjected to fitting with various kinetic models. The *in vitro* release data indicated that the drug release from the phytosomal formulation

adhered to first-order kinetics, with a Fickian model suggesting that the release process was diffusion-controlled fig. 5 [31].

The *in vitro* drug release from GPs exhibited a range spanning from $82.45 \pm 0.36\%$ to $92.07 \pm 0.83\%$ for formulations F2 through F17, respectively. The polynomial equation generated through the BBD for DR is as follows:

$$Y_2 = 91.07 + 1.29 X_1 + 1.95 X_2 + 1.17 X_3 + 0.44 X_1 X_2 - 1.58 X_1 X_3 - 0.07 X_2 X_3 - 2.86 X_1^2 - 0.35 X_2^2 - 1.59 X_3^2 \dots\dots (4)$$

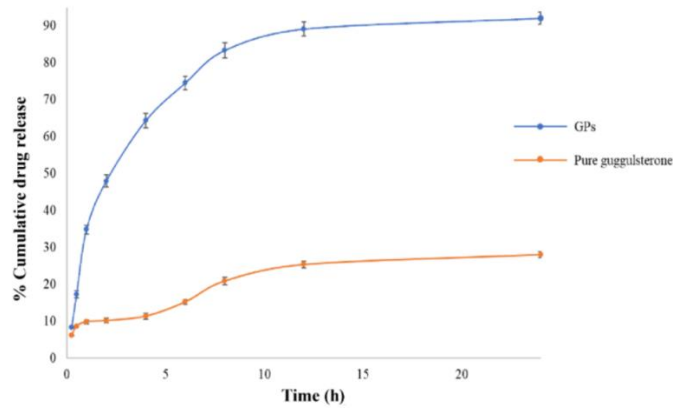


Fig. 5: Release pattern of GPs and pure guggulsterone, data presented are means±SD of triplicate experiment (n=3)

The *p*-value for drug release was found to be less than 0.0001, and the *F* ratio, which stood at 115.35, signified the model's significant relevance. Moreover, the R-squared (R^2) value of 0.9933 demonstrated an excellent fit of the model to the data. It's worth noting that the percentage of DR exhibited only a modest susceptibility to the variations in the independent variables. The influence of these factors on DR is visually represented through the utilization of three-dimensional response surface plots and two-dimensional contour plots, as presented in fig. 6.

Optimization

The effects of factors on desired responses (EE and DR) of 17 formulations are shown in table 1. The utilization of BBD for the design and optimization of GPs represented an effective and

systematic approach. It allowed for a comprehensive understanding of the influence of independent variables or factors on the selected responses (table 2). In the quadratic polynomial equations (Equations 3 and 4), the coefficients (X_1 , X_2 , and X_3) associated with a single factor were indicative of the primary effect (either Entrapment Efficiency or Drug Release) of that specific factor. Conversely, coefficients involving more than one factor were indicative of the interactions between those variables. A positive coefficient factor signified a direct relationship between the factor and the response, whereas a negative coefficient indicated the opposite effect. The two-dimensional and three-dimensional response surface graphs generated by the polynomial equations provided a visual representation of the concurrent impact of two variables on response parameters while maintaining one variable at a constant level [32, 33].

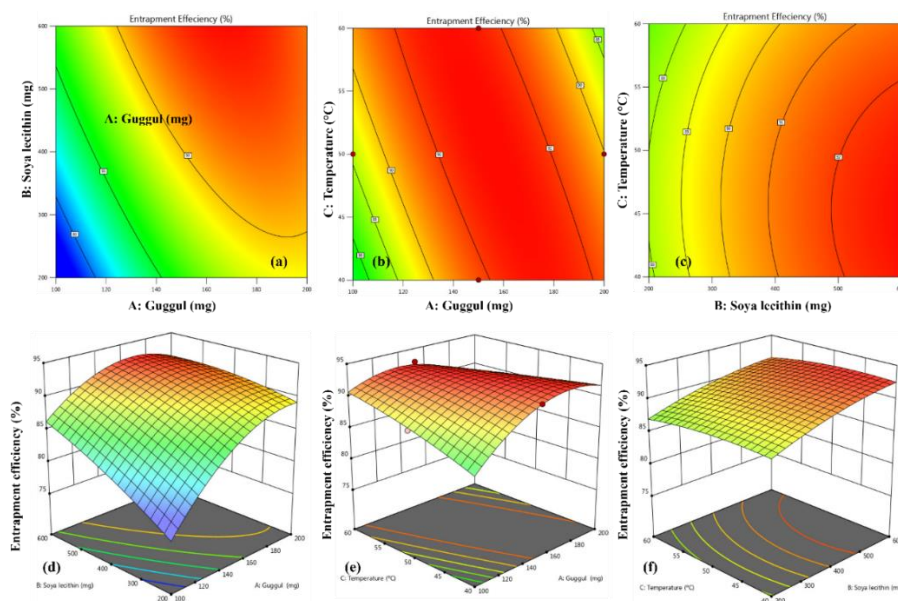


Fig. 6: 2D contour plots and 3D response surface plots of EE as a function of (a) and (d) guggulsterone and soy lecithin; (b) and (e) guggulsterone and temperature, and (c) and (f) soy lecithin and temperature

Table 2: Design of experiment factors, responses, and their levels

Factors	Coded levels of variables		
	Low (-1)	Medium (0)	High (+1)
Independent variables			
X ₁ = Guggul (mg)	100	150	200
X ₂ = Soy lecithin (mg)	200	400	600
X ₃ = Temperature (°C)	40	50	60
Dependent variables (Responses)			
Y ₁ = % Entrapment Efficiency (%EE)			Maximize
Y ₂ = % Drug Release (%DR)			Maximize

A linear increase in EE (Y₁) was observed as the concentration or dosage of guggulsterone (X₁) and soy lecithin (X₂) increased. This increase indicated that a higher amount of the drug was available for encapsulation. Furthermore, higher temperatures (X₃) favored greater EE, as depicted in fig. 7. In contrast to other lipid-based vesicular systems, this enhanced EE could be attributed to the fact that the bioactive phyto-constituents are an integral part of the vesicular membrane. They are anchored to the polar head of the phospholipid through a chemical (hydrogen) bond, rather than being simply entrapped within the aqueous core or phospholipid bilayers of the vesicular membrane [30]. A curvilinear increase in drug release (Y₂) was observed in response to factors X₁ and X₃, while a linear increase was evident with soy lecithin (X₂). During the checkpoint analysis, there was an outstanding agreement between the measured responses and the predicted values for both EE and DR. The experimental values closely aligned with the predicted values, displaying minimal percentage bias, which underscored the reliability of the employed mathematical model. Consequently, a numerical optimization technique utilizing a desirability approach was employed to optimize the GPs. The optimal concentrations of guggulsterone, soy lecithin, and temperature (X₁, X₂, and X₃) were determined to be 169.62 mg, 600 mg, and 42.63 °C, respectively. These values yielded promising and optimized phytosomes with an EE of 92.64% and a DR of 91.69% (over 24 h), achieving an overall desirability score of 0.986. The percentage probability plots, as depicted in fig. 7 (a and b) provide evidence that errors conform to a normal distribution and are devoid of interdependence while exhibiting uniform error variance. Additionally, the residual plots, presented in fig. 7 (c and d) reveal a random distribution of residuals without discernible trends, further affirming the model's ability to make accurate predictions with consistent variance. Lastly, the parity plots shown in fig. 7 (e and f) establish a correlation between the observed responses and the predictions generated by the models. A numerical optimization technique employing a desirability approach was implemented to optimize the GPs to maximize both the percentage of EE and DR. The optimized GPs were composed of specific quantities, specifically 169.62 mg of X₁, 600 mg of X₂, and a temperature of 42.63 °C for X₃, yielding the

desired responses of 92.64% for Y₁ and 91.69% for Y₂, with an overall desirability score of 0.986. Curved rise was seen in guggulsterone and temperature graph in terms of drug release, whereas the linear increase was seen in soya lecithin. The mathematical model was found to be reliable due to the high level of agreement between measured and anticipated values of EE and drug release. Promising phytosomes with high EE and DR % were resulted due to ideal concentration of guggulsterone, 2D contour plots, 3D response surface plots, % probability plots, residual plots, and parity plots was visualised and validated for data, which showed a link between observed responses and model predictions. Overall, the GPs were successfully adjusted to optimise both DR and EE, resulting in high desirability scores and demonstrating the effectiveness of BBD in pharmaceutical formulation design and optimization [34].

Stability studies

During stability studies, the optimized GPs demonstrated stability and retained their structural integrity under various stress conditions, as corroborated by the FTIR spectral analysis. This improved stability could potentially be attributed to the formation of chemical bonds between the polar head of the amphiphile molecule and the phytoconstituent. Furthermore, the optimized GPs exhibited a faster absorption rate, which could potentially lead to a reduced required dosage of the drug to achieve the desired pharmacological effect. The physical appearance of GPs formulation stored at 4 °C and 24 °C for 1, 2, and 3 mo was evaluated. At the end of 1, 2, and 3 mo, GPs stored at 4 °C and 24 °C were stable. The data from stability studies indicated that there were no observable physicochemical alterations in the GPs, and there was no discernible shift in the primary functional groups of guggulsterone, as evidenced by the FTIR spectra presented in fig. 8. Furthermore, the optimized formulations, when subjected to various stress conditions, did not manifest any changes in terms of their physicochemical integrity, drug content (maintaining a level of 92.54%), or drug release (which ranged from 88.61% to 90.38% over 24 h). Consequently, it can be concluded that the optimized GPs remained physicochemically stable throughout the stability assessment.

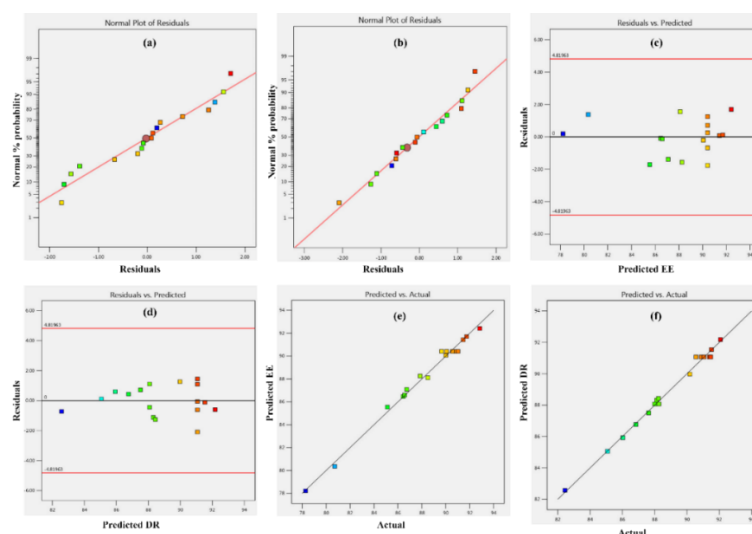


Fig. 7: (a, b) Normal percentage probability, (c, d) residual plots, and (e, f) parity charts of predicted versus actual responses for EE and DR

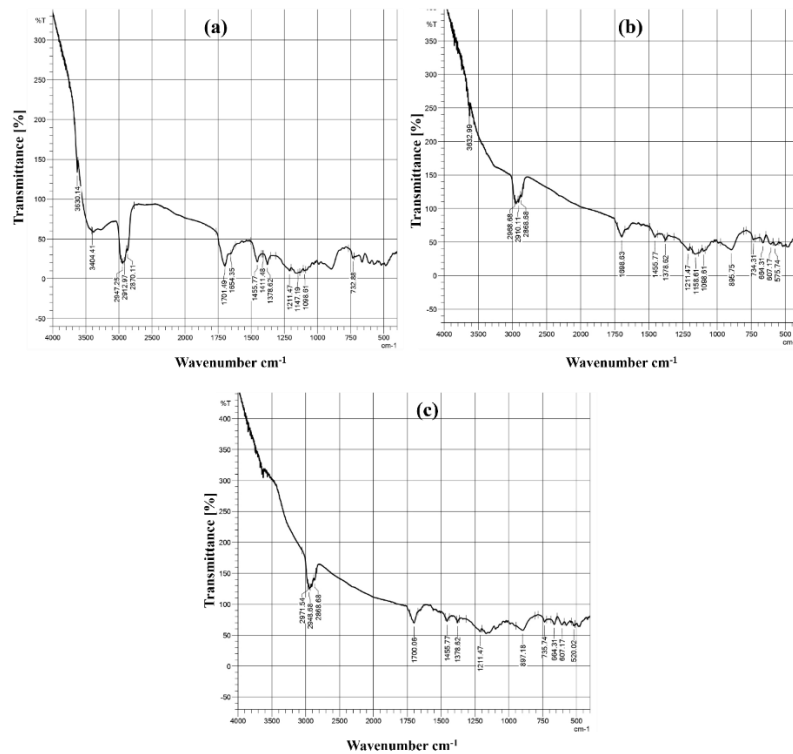


Fig. 8: FTIR of optimized GPs at (a) 30th d, (b) 60th d, and (c) 90th d

Apparent water solubility

A drug's solubility is one of the main variables affecting its bioavailability following oral administration. Since solubility restricts the amount of drug that can pass through the stomach-intestinal barrier during oral absorption, it is essential to measure and verify that the appropriate dosage of medication is being taken. Water makes up a large portion of all body fluids. Any medication administered to the body needs to have the highest possible water solubility in order to be therapeutically effective. Substances that are

somewhat insoluble therefore, exhibit insufficient absorption. In the current study, the solubility of guggulsterone (GS), guggulsterone phytosomes (GPs), and the soy lecithin (GS-SL) combination in an aqueous medium were evaluated. Table 3 shows that GPs solubility (84.3±0.065µg/ml) was significantly higher than that of GS (12.2 ±0.061µg/ml) and the GS-SL physical mixture (36.7±0.073 µg/ml). It can be inferred that the phytosome complex approach improved the solubility of weakly water-soluble guggulsterone due to the complex's amorphous nature and soyalecithin's ability to form micelles in aqueous solution [11].

Table 3: Solubility of GS, mixture of GS and SL, and GPs in distilled water

S. No.	Sample	Aqueous solubility µg/ml
1	Guggulsterone (GS)	12.2 ±0.061
2	Guggulsterone-Soy lecithin mixture (GS-SL)	36.7±0.073
3	Guggulsterone Phytosomes (GPs)	84.3±0.065

*Data presented are means±SD of triplicate experiment (n=3).

Apparent octanol-water partition coefficient

The apparent division coefficient (Log P) measures the hydrophilicity/lipophilicity and absorption capacity of a compound [35]. The Log P values mainly affect biological characteristics such as bioaccumulation and toxicity. An important factor in membrane permeability is the partition coefficient. Drugs with high partition

coefficients can easily pass through the biological membrane. Many studies show that drugs with P logs between 1 and 2 are easy to absorb [36]. In the phosphate buffers with different pH values, the log P of GS was less than 1, showing a low absorption and permeability. In table 4, the log P values generated by the GPs in various buffers compared to GS are shown. This improvement could be attributed to the polar groups [11].

Table 4: Apparent octanol–water partition coefficient (Log P Value) of GS and GPs complex

Solvent	Log P value*	
	GS	GPs
pH 1.2 hydrochloric acid	0.8155±0.02	1.706±0.01
Distilled water (pH 5.6)	0.6922±0.01	1.602±0.01
pH 6.8 phosphate buffer	0.5070±0.009	1.564±0.002
pH 7.5 phosphate buffer	0.3422±0.004	1.311±0.004

*Data presented are means±SD of triplicate experiment (n=3).

In vitro cell line study (MTT assay)

The optimized GPs exhibited a superior level of cell viability when assessed across three selected cell lines. Specifically, the cell viability function, denoted by CTC₅₀ values, for GPs was determined to be 251.18 µg/ml, 206.35 µg/ml, and 311.61 µg/ml for the MF 3T3-L1, MCF-12A, and NSC-34 cells, respectively. In comparison, pure guggulsterone demonstrated CTC₅₀ values of 264.70 µg/ml, 253.39 µg/ml, and 330.44 µg/ml for the same cell lines, namely MF 3T3-L1, MCF-12A, and NSC-34 cells, respectively. Notably, the optimized GPs were found to be compatible and viable when assessed against 3T3-L1 mouse fibroblasts, mice motor neuron-like cells, and Vero cells, performing comparably to the pure form of guggulsterone. Importantly, these GPs did not exhibit any interfering or inhibitory effects on the reduction of MTT, further emphasizing their compatibility and safety profile [37].

CONCLUSION

The solvent evaporation technique is employed in the preparation of GPs. BBD is practiced to achieve desired experimental runs for optimization to cut short the wide range of experimental runs. The regression coefficients established by the second-order polynomial equations of all the responses indicated that the model is significant. Counter plots showed that the quadratic model generated was well-matched to all aspects of the experimental design. The optimized formulation showcased a remarkable entrapment efficiency of 92.64% and a drug release rate of 91.69% at 24 h FTIR studies revealed compatibility among the drug and excipients; XRD studies stated the preservation of guggulsterone's structural integrity within the GPs. The particle size of the optimized formulation was measured to be 137.8 nm, substantiating that the nanoparticles are in the nano range. Zeta potential recorded at -25.3 mV inferred the superlative stability of the optimized formulation. TEM analyses illustrated that optimized are spherical and homogeneous with minimum aggregation. Accelerated stability studies performed on the optimized formulation stated that there was no substantial variation in appearance and % DR. The optimized formulation displayed heightened viability in selected cell lines, exhibiting CTC with CTC₅₀ ranging from 253.39 to 330.44 µg/ml. GPs hold great potential as an innovative drug delivery carrier for delivering natural bioactive compounds, thereby enhancing their antihyperlipidemic properties. These formulations hold great promise as novel drug delivery carriers. They offer significant potential for improving the treatment of obesity and hyperlipidemia.

ACKNOWLEDGMENT

The authors thank the SRM College of Pharmacy, SRMIST, for providing tremendous opportunities to accomplish this work.

FUNDING

The authors declare that no funds, grants, or other support were received during the preparation of this manuscript.

ABBREVIATIONS

2D-two dimensional, 3D-three dimensional, ANOVA-Analysis of variance, BAR – Bile Acid Regulation, BBD-Box Behnken Design, CQAs – Critical Quality Attributes, CTCs – Circulating Tumor Cells, CYP7A1-Cholesterol 7 alpha-hydroxylase, DMEM-Dulbecco's modified eagle's medium, DMSO-Dimethyl Sulfoxide, DoE-Design of Experiments, DR-Drug Release, DSC-differential scanning calorimeter, EE-Entrapment efficiency, FBS-Fetal bovine serum, FT-IR-Fourier Transform Infrared, FXR-farnesoid X receptor, GS – Guggulsterone GPs – Guggulsterone Phytosomes, SL-Soy lecithin HL-Hyperlipidemia, IBMX-3-isobutyl-1-methylxanthine, KBr-Potassium bromide, MTT-3-(4, 5-dimethylthiazol-2-yl)-2, 5-diphenyltetrazolium, NPs-Polymeric Nanoparticles, SD-standard deviation, TEM-Transmission electron microscope, SLNs-Solid Lipid Nanoparticles, UV-Ultra Visible, XRD-X-ray diffraction, QbD-Quality by Design, PC-Phosphatidylcholine, MWCO-Molecular Weight Cut-Off, ICH-International Conference on Harmonization, BCS – Bovine Calf Serum.

AUTHORS CONTRIBUTIONS

Jamal Basha Dudekula: Conceptualization and Writing-Original Draft; Jebastin Koilpillai: Writing-Review and Editing; Damodharan

Narayanasamy: Writing-Review and Supervising. All authors read and approved the final manuscript.

CONFLICT OF INTERESTS

The authors have no relevant financial or non-financial interests to disclose.

REFERENCES

- Feynman RP. There's plenty of room at the bottom an invitation to enter a new field of physics. *Eng Sci Mag Cal Inst Technol.* 1960;23(22):1-7.
- Yusuf A, Almotairy AR, Henidi H, Alshehri OY, Aldughaim MS. Nanoparticles as drug delivery systems: a review of the implication of nanoparticles physicochemical properties on responses in biological systems. *Polymers.* 2023 Jan;15(7):1596. doi: [10.3390/polym15071596](https://doi.org/10.3390/polym15071596), PMID [37050210](https://pubmed.ncbi.nlm.nih.gov/37050210/).
- Shriram RG, Moin A, Alotaibi HF, Khafagy ES, Al Saqr A, Abu Lila AS. Phytosomes as a plausible nano delivery system for enhanced oral bioavailability and improved hepatoprotective activity of silymarin. *Pharmaceuticals (Basel).* 2022 Jun 24;15(7):790. doi: [10.3390/ph15070790](https://doi.org/10.3390/ph15070790), PMID [35890088](https://pubmed.ncbi.nlm.nih.gov/35890088/).
- Swain B, Koilpillai J, Narayanasamy D. Systematic review on recent advancements and liposomal technologies to develop stable liposome. *Curr Trends Biotechnol Pharm.* 2023 Feb 20;17(1):735-48. doi: [10.5530/ctbp.2023.1.13](https://doi.org/10.5530/ctbp.2023.1.13).
- Alharbi WS, Almughem FA, Almeahmady AM, Jarallah SJ, Alsharif WK, Alzahrani NM. Phytosomes as an emerging nanotechnology platform for the topical delivery of bioactive phytochemicals. *Pharmaceutics.* 2021 Sep 15;13(9):1475. doi: [10.3390/pharmaceutics13091475](https://doi.org/10.3390/pharmaceutics13091475), PMID [34575551](https://pubmed.ncbi.nlm.nih.gov/34575551/).
- Barani M, Sangiovanni E, Angarano M, Rajizadeh MA, Mehrabani M, Piazza S. Phytosomes as innovative delivery systems for phytochemicals: a comprehensive review of literature. *Int J Nanomedicine.* 2021;16:6983-7022. doi: [10.2147/IJN.S318416](https://doi.org/10.2147/IJN.S318416), PMID [34703224](https://pubmed.ncbi.nlm.nih.gov/34703224/).
- Lu M, Qiu Q, Luo X, Liu X, Sun J, Wang C. Phyto phospholipid complexes (phytosomes): a novel strategy to improve the bioavailability of active constituents. *Asian J Pharm Sci.* 2019 May;14(3):265-74. doi: [10.1016/j.ajps.2018.05.011](https://doi.org/10.1016/j.ajps.2018.05.011), PMID [32104457](https://pubmed.ncbi.nlm.nih.gov/32104457/).
- Jebastin K, Narayanasamy D. Rationale utilization of phospholipid excipients: a distinctive tool for progressing state of the art in research of emerging drug carriers. *J Liposome Res.* 2023 Mar;33(1):1-33. doi: [10.1080/08982104.2022.2069809](https://doi.org/10.1080/08982104.2022.2069809), PMID [35543241](https://pubmed.ncbi.nlm.nih.gov/35543241/).
- Chi C, Zhang C, Liu Y, Nie H, Zhou J, Ding Y. Phytosome nanosuspensions for silybin phospholipid complex with increased bioavailability and hepatoprotection efficacy. *Eur J Pharm Sci.* 2020 Mar 1;144:105212. doi: [10.1016/j.ejps.2020.105212](https://doi.org/10.1016/j.ejps.2020.105212), PMID [31923602](https://pubmed.ncbi.nlm.nih.gov/31923602/).
- Telange DR, Patil AT, Pethe AM, Fegade H, Anand S, Dave VS. Formulation and characterization of an apigenin phospholipid phytosome (APLC) for improved solubility *in vivo* bioavailability and antioxidant potential. *Eur J Pharm Sci.* 2017 Oct 15;108:36-49. doi: [10.1016/j.ejps.2016.12.009](https://doi.org/10.1016/j.ejps.2016.12.009), PMID [27939619](https://pubmed.ncbi.nlm.nih.gov/27939619/).
- Zeng Q Ping, Liu Z Hong, Huang A Wen, Zhang J, Song H Tao. Preparation and characterization of silymarin synchronized release microporous osmotic pump tablets. *Drug Des Dev Ther.* 2016 Jan 29;10:519-31. doi: [10.2147/DDDT.S91571](https://doi.org/10.2147/DDDT.S91571), PMID [26889080](https://pubmed.ncbi.nlm.nih.gov/26889080/).
- Vargas Mendoza N, Madrigal Santillan E, Morales Gonzalez A, Esquivel Soto J, Esquivel Chirino C, Garcia Luna Y, Gonzalez Rubio M. Hepatoprotective effect of silymarin. *World J Hepatol.* 2014;6(3):144-9. doi: [10.4254/wjh.v6.i3.144](https://doi.org/10.4254/wjh.v6.i3.144), PMID [24672644](https://pubmed.ncbi.nlm.nih.gov/24672644/).
- Surwase SS, Munot NM, Idage BB, Idage SB. Tailoring the properties of mPEG-PLLA nanoparticles for better encapsulation and tuned release of the hydrophilic anticancer drug. *Drug Deliv Transl Res.* 2017 Jun;7(3):416-27. doi: [10.1007/s13346-017-0372-9](https://doi.org/10.1007/s13346-017-0372-9), PMID [28324320](https://pubmed.ncbi.nlm.nih.gov/28324320/).
- Alshahrani SM. Optimization and characterization of cuscuta reflexa extract loaded phytosomes by the box behnken design to improve the oral bioavailability. *J Oleo Sci.* 2022 Apr 29;71(5):671-83. doi: [10.5650/jos.ess21318](https://doi.org/10.5650/jos.ess21318), PMID [35387912](https://pubmed.ncbi.nlm.nih.gov/35387912/).

15. Yanyu X, Yunmei S, Zhipeng C, Qineng P. The preparation of silybin-phospholipid complex and the study on its pharmacokinetics in rats. *Int J Pharm*. 2006 Jan 3;307(1):77-82. doi: [10.1016/j.ijpharm.2005.10.001](https://doi.org/10.1016/j.ijpharm.2005.10.001), PMID [16300915](https://pubmed.ncbi.nlm.nih.gov/16300915/).
16. Blackburn GL, Wollner S, Heymsfield SB. Lifestyle interventions for the treatment of class III obesity: a primary target for nutrition medicine in the obesity epidemic. *Am J Clin Nutr*. 2010 Jan 1;91(1):289S-92S. doi: [10.3945/ajcn.2009.28473D](https://doi.org/10.3945/ajcn.2009.28473D), PMID [19906805](https://pubmed.ncbi.nlm.nih.gov/19906805/).
17. Shattat GF. A review article on hyperlipidemia: types, treatments and new drug targets. *Biomed Pharmacol J*. 2014;7(2):399-409. doi: [10.13005/bpj/504](https://doi.org/10.13005/bpj/504).
18. Rupasinghe HP, Sekhon Loodu S, Mantso T, Panayiotidis MI. Phytochemicals in regulating fatty acid β -oxidation: potential underlying mechanisms and their involvement in obesity and weight loss. *Pharmacol Ther*. 2016 Sep;165:153-63. doi: [10.1016/j.pharmthera.2016.06.005](https://doi.org/10.1016/j.pharmthera.2016.06.005), PMID [27288729](https://pubmed.ncbi.nlm.nih.gov/27288729/).
19. Sinal CJ, Gonzalez FJ. Guggulsterone: an old approach to a new problem. *Trends Endocrinol Metab*. 2002 Sep;13(7):275-6. doi: [10.1016/s1043-2760\(02\)00640-9](https://doi.org/10.1016/s1043-2760(02)00640-9), PMID [12163224](https://pubmed.ncbi.nlm.nih.gov/12163224/).
20. Deng R. Therapeutic effects of guggul and its constituent guggulsterone: cardiovascular benefits. *Cardiovasc Drug Rev*. 2007;25(4):375-90. doi: [10.1111/j.1527-3466.2007.00023.x](https://doi.org/10.1111/j.1527-3466.2007.00023.x), PMID [18078436](https://pubmed.ncbi.nlm.nih.gov/18078436/).
21. Urizar NL, Moore DD. Gugulipid: a natural cholesterol lowering agent. *Annu Rev Nutr*. 2003;23:303-13. doi: [10.1146/annurev.nutr.23.011702.073102](https://doi.org/10.1146/annurev.nutr.23.011702.073102), PMID [12626688](https://pubmed.ncbi.nlm.nih.gov/12626688/).
22. Rathee S, Kamboj A. Optimization and development of antidiabetic phytosomes by the box-behnken design. *J Liposome Res*. 2018;28(2):161-72. doi: [10.1080/08982104.2017.1311913](https://doi.org/10.1080/08982104.2017.1311913), PMID [28337938](https://pubmed.ncbi.nlm.nih.gov/28337938/).
23. Martinez Ballesta M, Gil-Izquierdo A, Garcia Viguera C, Dominguez Perles R. Nanoparticles and controlled delivery for bioactive compounds: outlining challenges for new smart foods for health. *Foods*. 2018 May;7(5):72. doi: [10.3390/foods7050072](https://doi.org/10.3390/foods7050072), PMID [29735897](https://pubmed.ncbi.nlm.nih.gov/29735897/).
24. Govindaram LK, Bratty MA, Alhazmi HA, Kandasamy R, Thangavel N, Ibrahim AM. Formulation biopharmaceutical evaluation and *in vitro* screening of polyherbal phytosomes for breast cancer therapy. *Drug Dev Ind Pharm*. 2022 Oct;48(10):552-65. doi: [10.1080/03639045.2022.2138911](https://doi.org/10.1080/03639045.2022.2138911), PMID [36269296](https://pubmed.ncbi.nlm.nih.gov/36269296/).
25. Setiadi S, Hidayah N. The effect of papain enzyme dosage on the modification of egg yolk lecithin emulsifier product through enzymatic hydrolysis reaction. *I J Tech*. 2018;9(2):380-9. doi: [10.14716/ijtech.v9i2.1073](https://doi.org/10.14716/ijtech.v9i2.1073).
26. Ittadwar PA, Puranik PK. Novel umbelliferone phytosomes: development and optimization using experimental design approach and evaluation of photo-protective and antioxidant activity. *Int J Pharm Pharm Sci*. 2017 Jan 1;9(1):218-28. doi: [10.22159/ijpps.2017v9i1.14635](https://doi.org/10.22159/ijpps.2017v9i1.14635).
27. B JJ, KR. Development and *in vitro* evaluation of phytosomes of ellagic acid. *Asian J Pharm Clin Res*. 2023 Mar 7;16(3):105-9. doi: [10.22159/ajpcr.2023.v16i3.47129](https://doi.org/10.22159/ajpcr.2023.v16i3.47129).
28. Haider T, Pandey V, Behera C, Kumar P, Gupta PN, Soni V. Spectrin conjugated PLGA nanoparticles for potential membrane phospholipid interactions: development optimization and *in vitro* studies. *J Drug Deliv Sci Technol*. 2020 Dec;60:102087. doi: [10.1016/j.jddst.2020.102087](https://doi.org/10.1016/j.jddst.2020.102087).
29. Zaki RM, Ali AA, El Menshawe SF, Bary AA. Formulation and *in vitro* evaluation of diacerein loaded niosomes. *Int J Pharm Pharm Sci*. 2014;6(Suppl 2):515-21.
30. Udupurkar PP, Bhusnure OG, Kamble SR. Diosmin phytosomes: development optimization and physicochemical characterization. *IJPER*. 2018 Aug 1;52(4s):s29-36. doi: [10.5530/ijper.52.4s.73](https://doi.org/10.5530/ijper.52.4s.73).
31. Costa P, Sousa Lobo JM. Modeling and comparison of dissolution profiles. *Eur J Pharm Sci*. 2001 May 1;13(2):123-33. doi: [10.1016/s0928-0987\(01\)00095-1](https://doi.org/10.1016/s0928-0987(01)00095-1), PMID [11297896](https://pubmed.ncbi.nlm.nih.gov/11297896/).
32. Shaikh AA, Chaudhari PD, Holkar SS. A design of experiment approach for optimization and characterization of etodolac ternary system using spray drying. *Int J Pharm Pharm Sci*. 2017 Feb 1;9(2):233-40. doi: [10.22159/ijpps.2017v9i2.16087](https://doi.org/10.22159/ijpps.2017v9i2.16087).
33. B JJ, P MR. Development and *in vitro* evaluation of phytosomes of naringin. *Asian J Pharm Clin Res*. 2019 Sep 7;12(9):252-6. doi: [10.22159/ajpcr.2019.v12i9.34798](https://doi.org/10.22159/ajpcr.2019.v12i9.34798).
34. Koilpillai J, Narayanasamy D. Development and characterization of novel surface engineered depofom: a QBD coupled failure modes and effects analysis risk assessment based optimization studies. *J Liposome Res*. 2024;34(1):1-17. doi: [10.1080/08982104.2023.2208662](https://doi.org/10.1080/08982104.2023.2208662), PMID [37144416](https://pubmed.ncbi.nlm.nih.gov/37144416/).
35. Cumming H, Rucker C. Octanol water partition coefficient measurement by a simple ^1H NMR method. *ACS Omega*. 2017 Sep 30;2(9):6244-9. doi: [10.1021/acsomega.7b01102](https://doi.org/10.1021/acsomega.7b01102), PMID [31457869](https://pubmed.ncbi.nlm.nih.gov/31457869/).
36. Papich MG, Martinez MN. Applying biopharmaceutical classification system (BCS) criteria to predict oral absorption of drugs in dogs: challenges and pitfalls. *AAPS J*. 2015 Jul;17(4):948-64. doi: [10.1208/s12248-015-9743-7](https://doi.org/10.1208/s12248-015-9743-7), PMID [25916691](https://pubmed.ncbi.nlm.nih.gov/25916691/).
37. Sedky NK, Braoudaki M, Mahdy NK, Amin K, Fawzy IM, Eftimiadou EK. Box-behnken design of thermo responsive nano liposomes loaded with a platinum(IV) anticancer complex: evaluation of cytotoxicity and apoptotic pathways in triple negative breast cancer cells. *Nanoscale Adv*. 2023 Sep 26;5(19):5399-413. doi: [10.1039/D3NA00368J](https://doi.org/10.1039/D3NA00368J), PMID [37767043](https://pubmed.ncbi.nlm.nih.gov/37767043/).